Available online at www.sciencedirect.com
ScienceDirect
International Journal of Mass Spectrometry 267 (2007) 256–262
International Journal of Mass Spectrometry
www.elsevier.com/locate/ijms

An investigation of the dissociation of complexes of triethylene tetramine with first-row transition-metal dications by electrospray ionization tandem mass spectrometry: Remote C–C bond activation

Janna Anichina, Diethard K. Bohme *

Department of Chemistry and Centre for Research in Mass Spectrometry, York University, 4700 Keele Street, Toronto, Ontario, Canada M3J 1P3

Received 16 November 2006; received in revised form 12 February 2007; accepted 21 February 2007
Available online 25 February 2007

Dedicated to Sharon Lias, in memory of her outstanding contributions to gas-phase ion chemistry and thermodynamics.

Abstract

Electrospray ionization mass spectrometry is employed to probe the complexation and dissociation of the first-row transition-metal dications with triethylene tetramine that originate in water/methanol solutions of the corresponding metal salts and the ligand. The major complex ions emerging from the ESI source were observed to be ML^{2+}, $ML(CH_3OH)^{2+}$, $M(L–H)^+$, $MLCl^+$ and $MLNO_3^+$ (M = Mn, Fe, Co, Ni, Cu, Zn and L = triethylene tetramine). Upon collision induced dissociation all dications, except those containing copper, exhibit the predominant loss of up to three hydrogen molecules. Remote C–C bond activation in the copper containing CuL^{2+} dication appears to be manifested by its heterolytic dissociation via charge separation into the two monocations $NH_2(CH_2)_2NHCH_2^+$ and $CuNH_2(CH_2)_2NHCH_2^+$ and this is attributed to the tendency for $Cu^{2+}(d^9)$ to achieve the $Cu^+(d^{10})$ configuration. The ion pairs $MLCl^+$ and $MLNO_3^+$ undergo exclusive elimination of the corresponding acid (HCl or HNO_3) to form $M(L–H)^+$ with the proton originating from one of the amino groups. The latter was demonstrated with CID experiments performed on deuterium labeled ion pair complexes. The onset energies for the loss of acid increase with decreasing IE(M^+) and this is in line with an increase in the endothermicity of the dissociation that is expected as the energy gained in the reduction of M^{2+} decreases. Further dissociation of $M(L–H)^+$ proceeds by loss of H_2, NH_3 and NH_2CH_2 radicals with all metals except Cu which loses NH_2CH_2 radicals exclusively.

Keywords: Transition-metal dications; Triethylene tetramine; Electrospray ionization; Collision-induced dissociation (CID); C–C bond activation

1. Introduction

Over the past decade electrospray ionization mass spectrometry (ESI–MS) has been successfully employed to investigate structural features, intrinsic stabilities and reactivities of multiply-charged coordination compounds of the first-row transition-metal dications [1–8]. Polyamino complexes of the latter have attracted attention due to the relatively high concentrations of polyamines in vivo where they are present as protonated or metallated complexes rather than as free ligands. Polyamino ligands are utilized in medicine for diagnostic imaging and in industry for the production of polymers [9,10]. Moreover, the study of low molecular weight transition-metal complexes is frequently of value in the elucidation of the chemistry of metalloproteins [11]. ESI/MS was used to prove the existence of a complex containing Cu and Zn dications in the environment of diethylenetriamine, deprotanated imidazole and tris(2-aminoethylamine) [12]. ESI/MS/MS also has been used to investigate the binding of Ag^+, Cu^+, Cu^{2+} and Pt^{2+} with polyamidoamine generation 1 amine terminated $PAMAMG1NH_2$ [13]. Triethylene tetramine, a member of the polyamine family, is particularly interesting due to the fact that it is used for the treatment of Wilson's disease, an autosomal recessive disorder characterized by copper accumulation in various organs, such as the liver, kidney and brain [14]. Despite the fact that all six of the doubly charged first-row transition-metal ions (Mn^{2+}, Fe^{2+}, Co^{2+}, Ni^{2+}, Cu^{2+} and Zn^{2+}) exhibit very high affinities toward triethylene tetramine in aqueous solution [15], the main competitors for the ligand in vivo are copper, zinc and iron [14]. In aqueous solutions triethylene tetramine behaves as a tetradentate ligand that

* Corresponding author. Tel.: +1 416 736 2100x66188; fax: +1 416 736 5936.
E-mail address: dkbohme@yorku.ca (D.K. Bohme).

1387-3806/$ – see front matter © 2007 Elsevier B.V. All rights reserved.
doi:10.1016/j.ijms.2007.02.043

is capable of forming four coordinative bonds with a metal ion through the lone pairs of its nitrogen atoms, two of which belong to the primary amino groups and the other two to the secondary ones. Metal ion–ligand coordination results in the formation of a 10-membered chelate ring [16].

Here we report the results of a study of the complexation of the doubly charged first-row transition-metal ions by triethylene tetramine in water–methanol solutions utilizing ESI–MS, including a comparative investigation of the gas-phase collision-induced dissociation (CID) pathways and stabilities of various other species either present in solution or formed as the result of electrospray ionization.

2. Experimental

Electrospray data were acquired in the positive ion mode using an API 2000 (MDS-SCIEX, Concord, Ont., Canada) triple quadrupole ($Q_1q_2Q_3$) mass spectrometer equipped with a "Turbo Ion Spray" ion source. Experiments were performed at an ion spray voltage of 5500 V, a ring-electrode potential of 300 V (used for ion beam confinement) and a range of potential differences between the orifice and the skimmer. N_2 was used as a curtain gas at a setting of 10 psi and air was used as a nebulizer at a flow rate of 8 L min^{-1}. Samples were directly infused into the electrospray source at a flow rate of 3 μL min^{-1}.

MS/MS was performed in the product ion and multiple reaction monitoring (MRM) modes with N_2 as collision gas at a pressure estimated to be about 3 mTorr (viz. multi-collision conditions). The collision offset voltage (the potential difference between the quadrupole entrance lens (q_0) and the collision cell quadrupole (q_2)), which nominally gives the laboratory frame collision energy, was adjusted between 5 and 130 V at 1 V intervals. Space charge and contact potentials, field penetration and field distortion all can influence the actual collision energy but were not taken into account. The zero of energy was not measured. Product ion spectra were then obtained by scanning Q_3 over the range m/z = 10–650. The inter-quadrupole lens potentials and the float potential of the resolving quadrupole Q_3 were linked to the q_2 potential to maintain proper transmission through Q_3.

The onset energy of a particular primary dissociation was determined by extrapolating the steepest slope of a plot of the sum of the relative intensities of the primary dissociation products and their further fragments (the "refined curve") versus the applied collision energy, to the x-axis, as shown in Fig. 1. The precision of the onset energies is taken to be one standard deviation from the mean onset energy value obtained in several (three or more) repeated experiments. In each experiment Gaussian smoothing was applied twice to the ion signals measured at each collision voltage, each accumulated for a dwell time of 200 ms, in order to remove local variations caused by noise. We have chosen this approach over reporting separately the onsets for individual primary product ions. The inclusion of the further dissociation product ions improves the determination of the onset energy, especially for those primary ions that quickly dissociate further. For primary dissociations leading to charge separation both primary product ions and their respective secondary and higher-order fragment ions (if any) are all added together. This approach is somewhat different from those reported previously, such as the $E_{1/2}$ method of David and Brodbelt [17] and the E_D (or tangent) and other methods described by Forbes et al. [18]. The onset energies were not measured as a function of pressure.

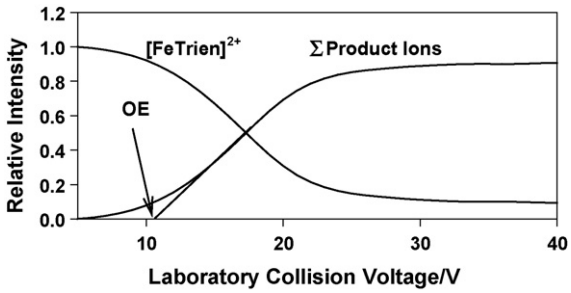

Fig. 1. Determination of the onset energy, OE, from the "refined curve" of the sum of the intensities of all the dissociation products in the collision-induced dissociation of the ligated metal dication $[FeTrien]^{2+}$.

Ligated Mn(II), Co(II), Ni(II), Cu(II) and Zn(II) were generated from their nitrate hydrates (Aldrich, p.a. ≥99.99%) while iron(II) sulfate heptahydrate (Aldrich, p.a. ≥98.%) was used as the source of Fe(II) ions; triethylenetetramine (Trien) hydrochloride was purchased from Aldrich p.a. ≥98.%. HPLC degree methanol and Millipore (18.2 mΩ) water were used to prepare the solvent mixture. The Trien was dissolved in a (1:1) water/methanol mixture at a concentration of 10 μM and the appropriate metal salt was added to five-fold molar excess.

3. Results and discussion

3.1. Ions emerging from the electrospray source

Five different types of metal complexes were observed to predominate in the electrospray of 50 μM solutions of the salts of doubly charged manganese, iron, cobalt, nickel, zinc and copper ions dissolved in (1:1) water/methanol mixtures containing

Table 1
Metal complex ions emerging from the ESI source of the API 2000 mass spectrometer at DP = 1–200 V[a]

	Mn	Fe	Co	Ni	Cu	Zn
ML^{2+}	21	32	13	31	23	15
$ML(CH_3OH)^{2+}$			12	6	12	
$MLNO_3^+$	31	16	6	11	19	
$MLCl^+$	29	30	22	17	18	39
$M(L–H)^+$	19	38	37	40	36	27

The relative abundances, averaged over the whole range of DP, are given in percentage with an estimated accuracy of 8% (they do not take into account other non-metallated ions).

[a] The samples were electrosprayed at concentration ratios of 5:1 metal ion:ligand with the concentration of the ligand = 10 μM from solutions of 1:1 water:methanol. Cu(II), Zn(II), Co(II), Ni(II) and Mn(II) were generated from their nitrate hydrates and Fe(II) from its sulfate heptahydrate. The triethyleneteramine ligand was utilized in the form of its hydrochloride.

10 μM triethylenetetramine (Trien). These are summarized in Table 1. The relative intensities of the complexes vary as a function of the Declustering Potential (DP), the instrumental parameter that has the greatest effect on the fragmentation in the orifice—skimmer region of the electrospray ionization source. $[MTrien]^{2+}$ dications were found to predominate in the electrospray spectra of solutions of copper, nickel, iron and cobalt in the range of DP 0–30 V, while these were minor ions for M = Mn and Zn. The latter presumably is due to relatively low stability constants. For example, in the known case of Mn, the values of log *K* in aqueous solution for the equilibrium $M^{2+} + L \leftrightarrow ML^{2+}$ are 5, 7, 8, 11.3, 14.5 and 20 for Mn(II), Fe(II), Co(II), Ni(II) and Cu(II), respectively [15].

Two types of ion pairs, $[MTrienCl]^+$ with M = Mn, Fe, Co, Ni, Cu and Zn and $[MTrienNO_3]^+$ with M = Mn, Co, Ni, Cu and Zn, were observed to be present over the entire range of DP (0–200 V). These ion pairs presumably are formed in the electrospray process as ion concentrations in the droplets increase due to solvent evaporation. These ion pairs arise from the electrolytic dissociation of the metal salts and the Trien hydrochloride. The nitrate ion was not observed in the ESI spectrum of the iron containing system for which sulfate was used as the source of iron dications. $MLCl^+$ and $MLNO_3{}^+$ undergo elimination of the corresponding acid (HCl or HNO_3) to form $M(L–H)^+$. It is also interesting to note that the CH_3OH complexes, even when they are seen, are minor. They may be dissociating in the spray.

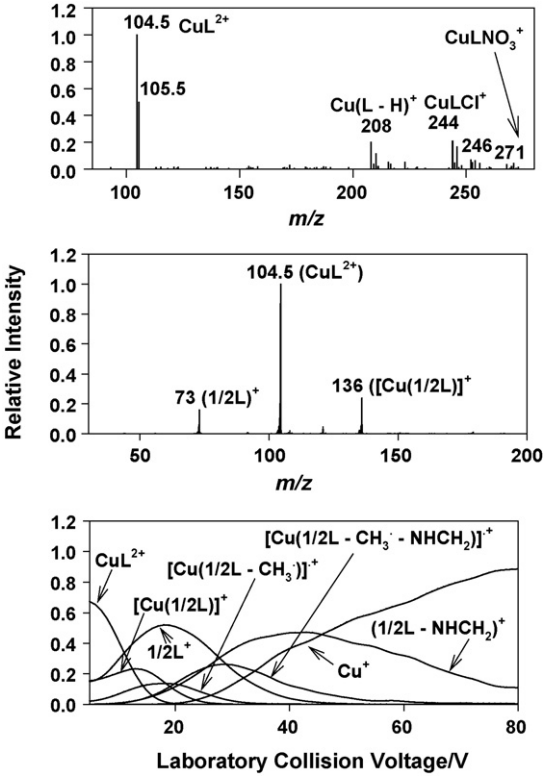

Fig. 2. (Top) ESI spectrum of the Cu(II) triethylene tetramine at DP = 0 V (L = triethylene tetramine). (Middle) CID spectrum of $m/z = 104.5$ (CuL^{2+}) at 5 V. (Bottom) CID profiles monitored for the dissociation of CuL^{2+}.

3.2. Fragmentation of metal–Trien species

3.2.1. Collision induced dissociation of $[CuTrien]^{2+}$

The CID of the $[CuTrien]^{2+}$ dication leads exclusively to charge separation with the formation of two singly charged species with *m/z* 73 and 136. The former corresponds to exactly half the mass of the neutral Trien molecule while the latter corresponds to the copper monocation attached to the other half of the Trien molecule (see Scheme 1 and Fig. 2). The accompanying C–C bond dissociation can be viewed to be heterolytic

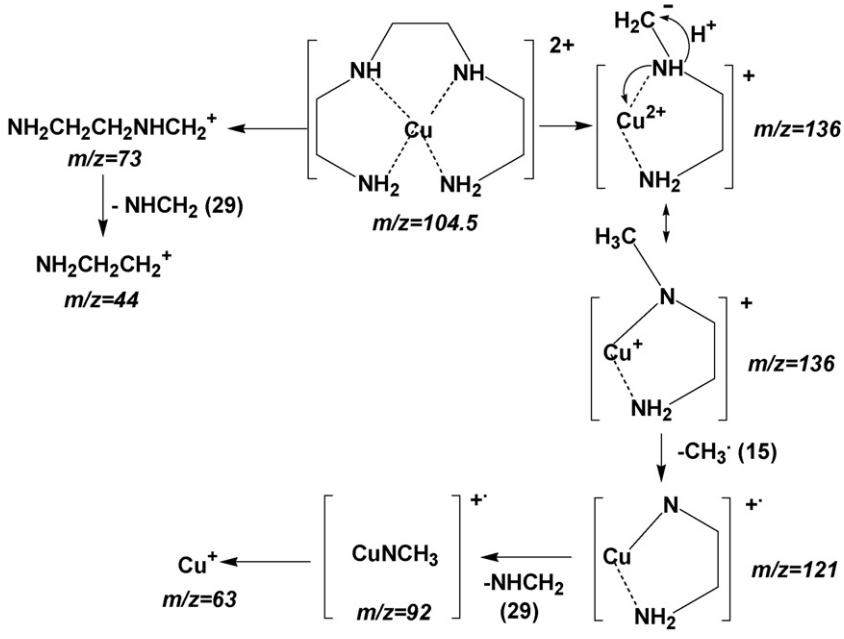

Scheme 1. Proposed mechanism for the dissociation of $[CuTrien]^{2+}$ via remote C–C bond activation.

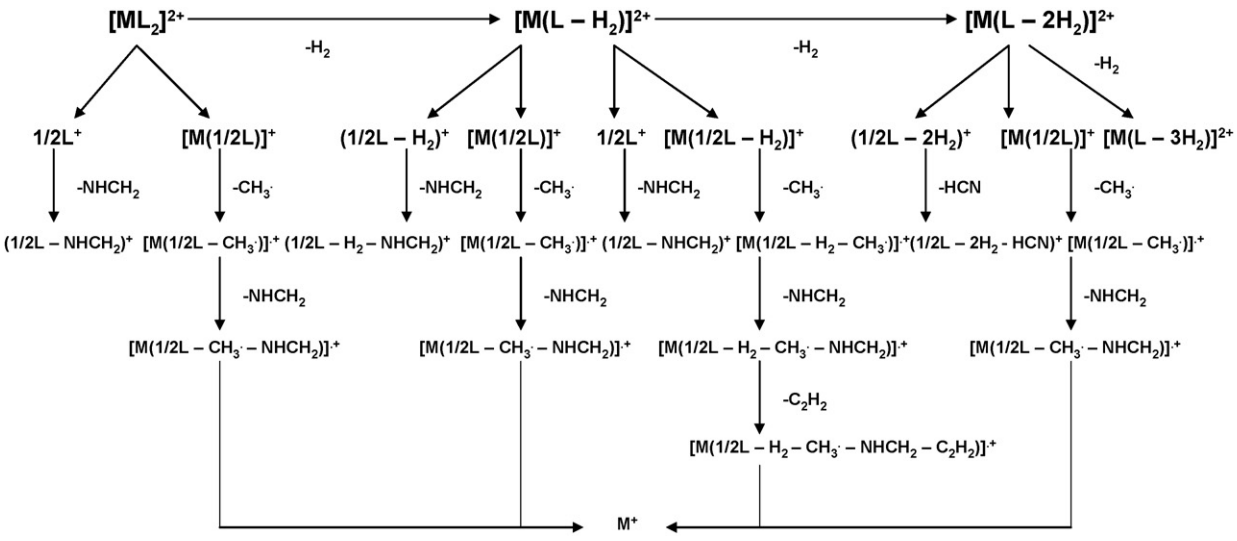

Scheme 2. Observed primary and higher-order dissociations of ML^{2+} with M = Mn, Fe, Co, Ni and Zn and L = triethylenetetramine.

and driven remotely by N–Cu^+ bond formation via a proton transfer from –NH– to $–CH_2^-$. The Cu^{2+} is reduced concomitantly by the transfer of an electron from –N– to Cu^{2+} which has a high electron recombination energy, IE(Cu^+) = 20.31 eV [19] and achieves a filled $Cu^+(d^{10})$ electronic configuration. Further fragmentation of both monocations takes place at elevated values of the laboratory collision energy and this is indicated in Scheme 1.

3.2.2. *Collision induced dissociation of $[MTrien]^{2+}$ with M = Mn, Fe, Co, Ni and Zn*

In contrast to the CID spectrum of the copper complex, Mn(II), Fe(II), Co(II), Ni(II) and Zn(II) containing complexes were observed to dissociate predominantly by the sequential loss of one, two and in some cases even three hydrogen molecules. The charge separation (C–C bond cleavage) channel seen with Cu(II) also was observed to compete, but only in a minor way: Mn(95:5), Fe(75:25), Co(95:5), Ni(95:5) and Zn(70:30). These branching ratios are estimated to have an accuracy within ±5%. These metals all have IE(M^+) < IE(Cu^+) and there is no strong correlation of the branching fraction for charge separation with the magnitude of IE(M^+).

The observed primary and higher-order dissociations are presented in Scheme 2. The dissociations of $[M(L–H_2)]^{2+}$ and $[M(L–2H_2)]^{2+}$ were measured separately. Fig. 3 provides experimental results obtained for the dissociations of $[CoL]^{2+}$, $[Co(L–H_2)]^{2+}$ and $[Co(L–2H_2)]^{2+}$. In each case the dissociation by H_2 loss was predominant but competed with one or two charge separation channels in a ratio of 95:5, 90:10 and 90:10, respectively.

CID experiments using the deuterium labeled triethylene tetramine ($ND_2(CH_2)_2ND(CH_2)_2ND(CH_2)_2ND_2$) revealed that the hydrogen atoms that are lost as molecular hydrogen originate from both the $–ND_2$ and $–CH_2$ substituents (Fig. 4).

The onset energies of the predominant dissociations of $[ML]^{2+}$ are given in Table 2. With the exception of the dissociation of $[NiL]^{2+}$, the onset energies increase with decreasing IE(M^+).

The methanol adduct ions $CoL(CH_3OH)^{2+}$, $NiL(CH_3OH)^{2+}$ and $FeL(CH_3OH)^{2+}$ were observed to lose methanol first upon CID and then to dissociate further in a manner observed for CoL^{2+}, NiL^{2+} and FeL^{2+}, respectively.

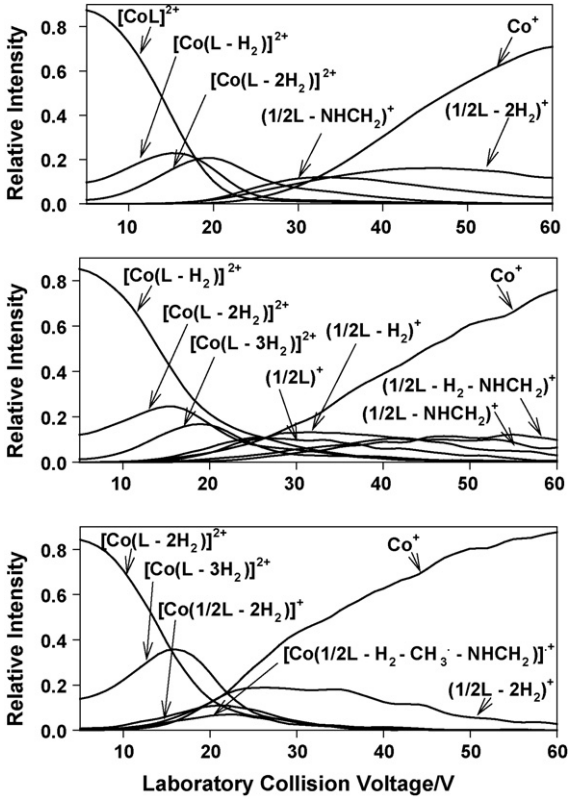

Fig. 3. CID profiles of the dissociation of $[CoL]^{2+}$ (upper spectrum), $[Co(L–H_2)]^{2+}$ (middle spectrum) and $[Co(L–2H_2)]^{2+}$ (bottom spectrum). The profiles of the ions whose intensities were smaller than 10% of the total intensity are not shown.

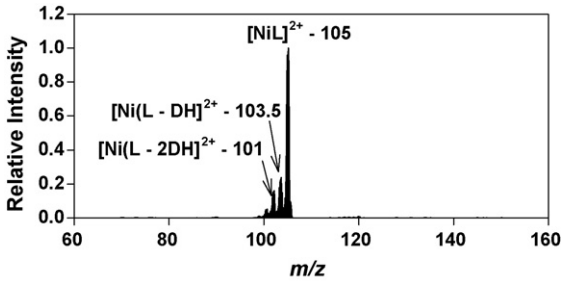

Fig. 4. CID spectrum of deuterated nickel(II)–Trien dication averaged for the 5–20 V range of the laboratory collision voltage.

3.3. Collision induced dissociation of the ion pairs $MLCl^+$ and $MLNO_3{}^+$

The monocations $[MTrienCl]^+$ and $[MTrienNO_3]^+$ were observed to dissociate exclusively by the loss of the corresponding acid, HCl and HNO_3, respectively, and formation of $M(Trien–H)^+$. CID experiments with deuterium labeled Trien demonstrated that the protons of both acids originate from the amino groups of the ligand.

Further analysis of the dissociation pattern of $Cu(Trien–D)^+$ suggests that the deuterium that is lost from the N-deuterated $[CuTrienCl]^+$ comes from the primary amino groups. This conclusion was reached on the basis of the higher-order dissociations that were observed and are indicated in Scheme 3. Loss of DX (where $X^- = NO_3{}^-$ or Cl^-) from copper-containing ion pairs leads to the formation of a fragment characterized by *m/z* 213 that corresponds to $[Cu(Trien–D)]^+$. The latter loses an $ND_2CH_2{}^{\cdot}$ radical producing a radical-cation of *m/z* = 181 whose dissociation continues in two competitive channels: $NDCH_2$ and $NDCHCH_2$ molecule losses. Neither of these reaction pathways would be possible if the protons in DX originated from one of the secondary amino groups (Scheme 3).

The secondary dissociation of $[M(L–H)]^+$ with M = Mn, Fe, Co, Ni and Zn that occurs after loss of acid corresponds to loss of H_2, loss of NH_3 and loss of $NH_2–CH_2$ radical and is followed by higher-order dissociations. Scheme 4 provides an overview of all the observed dissociations that were initiated by the dissociation of the ion pairs $MLCl^+$ and $MLNO_3{}^+$. Fig. 5 provides measured CID profiles for the dissociation of $NiLNO_3{}^+$.

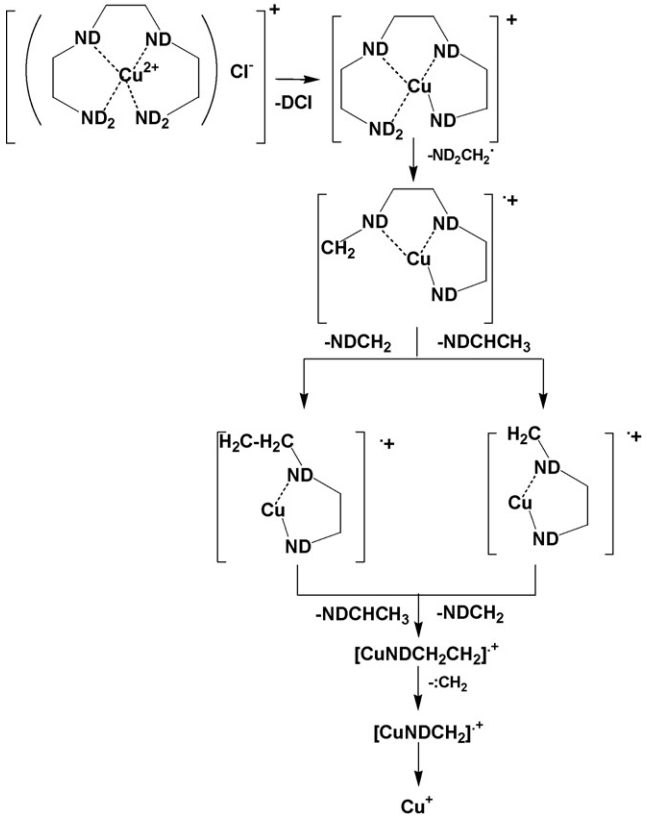

Scheme 3. Proposed mechanism for the dissociation of N-deuterated $[CuTrienCl]^+$.

The onset energies of the predominant dissociations of the ion pairs $[MLCl]^+$ and $[MLNO_3]^+$ are included in Table 2. Without exception within the uncertainty of the measurements, the onset energies for the loss of acid increase with decreasing $IE(M^+)$. This is in line with an increase in the endothermicity of the dissociation that is expected as the energy gained in the reduction of M^{2+} decreases.

Table 2
Measured onset energies for dissociation reactions (1), (2) and (3)

Metal	Reaction (1)		Reaction (2)		Reaction (3)		$IE(M^+)$[a]
	OE_{lab}[b]	OE_{CM}[c]	OE_{lab}[b]	OE_{CM}[c]	OE_{lab}[b]	OE_{CM}[c]	
Cu	6.3 ± 0.3	1.5	7.2 ± 0.2	0.7	6.1 ± 0.2	0.6	20.31
Ni	8.2 ± 0.3	1.2	7.9 ± 0.4	0.8	6.4 ± 0.3	0.6	18.17
Zn	7.3 ± 0.2	1.7	8.3 ± 0.2	0.8	6.9 ± 0.3	0.6	17.96
Co	9.6 ± 0.4	2.3	8.1 ± 0.4	0.8	7.8 ± 0.2	1.0	17.06
Fe	9.8 ± 0.3	2.4	12.5 ± 0.2	1.3	11.3 ± 0.3	1.1	16.18
Mn	10.1 ± 0.2	2.5	13.8 ± 0.3	1.5	12.5 ± 0.2	1.2	15.64

Reaction (1) $[CuL]^{2+} \rightarrow [Cu(1/2L)]^+ + (1/2L)^+$ and $[ML]^{2+} \rightarrow [M(L–H_2)]^{2+} + H_2$, where M = Mn, Fe, Co, Ni and Zn. Reaction (2) $[MLCl]^+ \rightarrow [M(L–H)]^+ + HCl$, where M = Mn, Fe, Co, Ni, Cu and Zn. Reaction (3) $[MLNO_3]^+ \rightarrow [M(L–H)]^+ + HNO_3$, where M = Mn, Co, Ni, Cu and Zn. Also given are the second ionization energies of the metals, $IE(M^+)$.

[a] Second ionization energy of the metal cation in eV [19].

[b] Measured onset energy in Volts.

[c] Apparent center-of-mass energy $OE_{CM} = OE_{lab} \times z \times m \times (m+M)^{-1}$, where *m* represents the mass of the collision gas (N_2) and *M* is that of the molecular ion investigated. *z* is the charge of the ion.

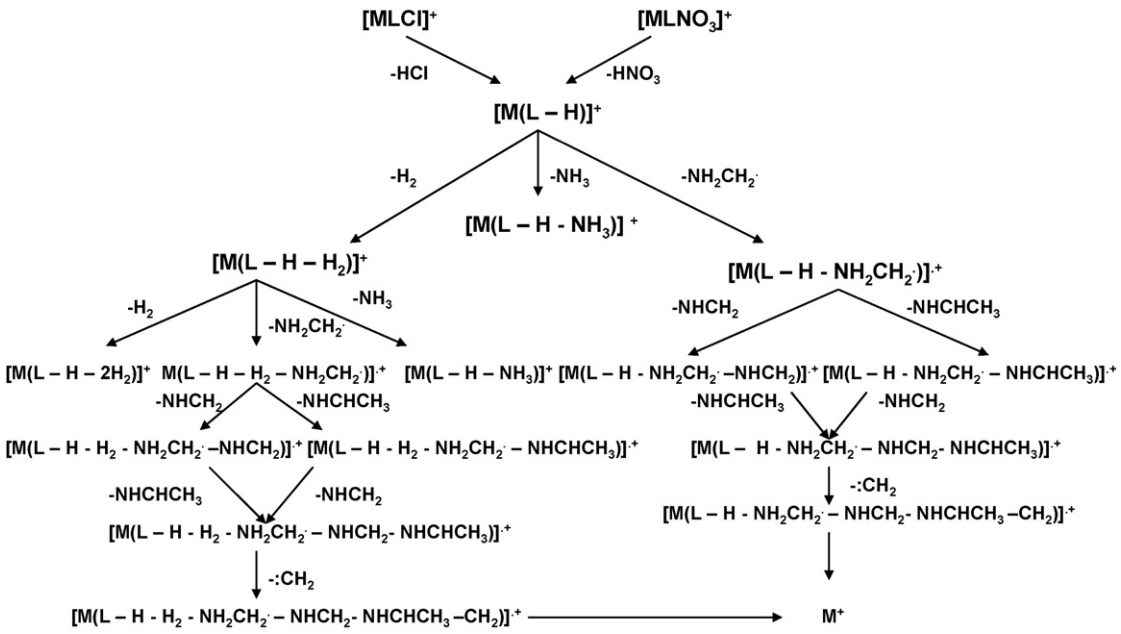

Scheme 4. Observed primary and higher-order dissociations of the ion pairs $MLCl^+$ and $MLNO_3{}^+$ with M = Mn, Fe, Co, Ni, Cu and Zn and L = triethylenetetramine.

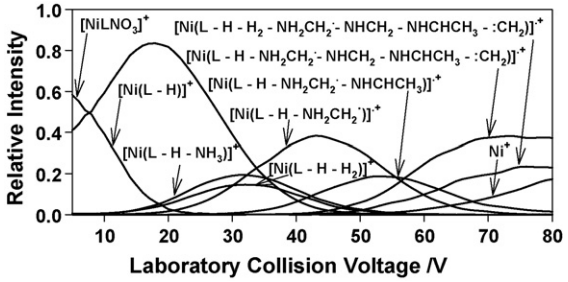

Fig. 5. CID profiles monitored for the dissociation of $NiLNO_3{}^+$. The profiles of the ions whose intensities were smaller than 10% of the total intensity are not shown.

4. Conclusions

Electrospraying solutions of triethylene tetramine and first-row transition-metal nitrates or sulfates provides a considerable variety of complexes of doubly charged first-row transition-metal cations ligated with Trien: $[MTrien]^{2+}$, $[MtrienCH_3OH]^{2+}$, $[M(Trien–H)]^+$, $[MTrienCl]^+$ and $[MTrienNO_3]^+$.

There is a uniformity in the CID of the mass-selected $[MTrien]^{2+}$ and $[M(Trien–H)]^+$ leading to the sequential loss of at least two hydrogen molecules by C–H and N–H activation that applies to all metal complexes except that containing Cu which prefer to dissociate by C–C bond cleavage. The heterolytic dissociation of CuL^{2+} via charge separation into the two monocations $NH_2(CH_2)_2NHCH_2{}^+$ and $CuNH_2(CH_2)_2NHCH_2{}^+$ may be attributed to the tendency for $Cu^{2+}(d^9)$ to achieve the $Cu^+(d^{10})$ configuration.

The ion pairs $MLCl^+$ and $MLNO_3{}^+$ undergo exclusive elimination of the corresponding acid (HCl or HNO_3) to form $M(L–H)^+$ with the proton originating from one of the amino groups. The onset energies for the loss of acid increase with decreasing $IE(M^+)$ and this is in line with an increase in the endothermicity of the dissociation that is expected as the energy gained in the reduction of M^{2+} decreases. Further dissociation of $M(L–H)^+$ proceeds by loss of H_2, NH_3 and NH_2CH_2 radicals with all metals except Cu which loses NH_2CH_2 radicals exclusively.

Acknowledgements

Continued financial support from the Natural Sciences and Engineering Research Council of Canada is greatly appreciated. Also, we acknowledge support from the National Research Council, the Natural Science and Engineering Research Council and MDS SCIEX in the form of a Research Partnership grant. As holder of a Canada Research Chair in Physical Chemistry, Diethard K. Bohme thanks the contributions of the Canada Research Chair Program to this research.

References

[1] J. Anichina, X. Zhao, D.K. Bohme, J. Phys. Chem. A 110 (2006) 10763.
[2] N. Tsierkezos, D. Schröder, H. Schwarz, Int. J. Mass Spectrom. 235 (2004) 33;
N.G. Tsierkezos, M. Diefenbach, D. Schröder, H. Schwarz, Inorg. Chem. 44 (2005) 4969.
[3] M. Alcami, A. Luna, O. Mo, M. Yanez, J. Tortajada, B. Amekraz, Chem. Eur. J. 10 (2004) 2927.
[4] M. Reyzer, J. Brodbelt, J. Am. Soc. Mass Spectrom. 11 (2000) 711.
[5] A.A. Shvartsburg, J. Am. Chem. Soc. 124 (2002) 12343.
[6] C.L. Gatlin, F. Turecek, T.J. Vaisar, J. Am. Chem. Soc. 117 (1995) 3637.
[7] M.Y. Combariza, A.M. Fahey, A. Milshteyn, R.W. Vachet, Int. J. Mass Spectrom. 244 (2005) 109.
[8] S.-S. Sun, A.J. Lees, Inorg. Chem. 40 (2001) 3154.
[9] D.P. Swanson, H.M. Chilton, J.H. Thrall, Pharmaceuticals in Medical Imaging, MacMillan Publishing Co. Inc., New York, 1989.
[10] R.M. Stephenson, J. Chem. Eng. Data 38 (1993) 634.
[11] J. Bridgewater, J. Lim, R.W. Vachet, Anal. Chem. 78 (7) (2006) 2432.

[12] A. Rockenbauer, Z. Kele, T. Kiss, J. Inorg. Biochem. 99 (2005) 1619.
[13] C.L. Mazzitelli, J.S. Brodbelt, J. Am. Soc. Mass Spectrom. 17 (2006) 676.
[14] H. Kodama, Y. Murata, T. Iitsuka, T. Abe, Life Sci. 61 (1997) 899; H. Kodama, in: L.W. Chang (Ed.), Toxicology of Metals, CRC Press, Boca Raton, 1996, p. 371.
[15] NIST Critical Stability Constants of Metal Complexes, Version 8, 2004.
[16] F.M. Doyle, Z. Liu, J. Colloid Interface Sci. 258 (2003) 396.
[17] W.M. David, J.S. Brodbelt, J. Am. Soc. Mass Spectrom. 14 (2003) 383.
[18] M.W. Forbes, D.A. Volmer, G.J. Francis, D.K. Bohme, J. Am. Soc. Mass Spectrom. 16 (2005) 779.
[19] http://webbook.nist.gov/chemistry/.